Supplemental Information

Materials and Methods

Redox titrations. A 4 ml solution of 40 μM FldA in 50 mM Tris-Cl pH 8.0 buffer was purged with nitrogen. In the anaerobic chamber, the following solutions of mediators were added to the final concentration of 10 μM: Phenazine methosulfate (80mV), thionine acetate (64mV), indigo carmine (-130mV), 2-hydroxy-1,4-naphthoquinone (-145mV), anthroquinone disulfonate (-170mV), sodium anthraquinone-2-sulfonate (-255mV), benzyl viologen (-358mV), methyl viologen (-440mV) and 1,1'-trimethylene-2,2'-dipyridinium dibromide (-521mV). Redox titrations were performed in a custom-made quartz cuvette transformed into a spectroelectrochemical cell containing a gold flag working electrode (Gauze electrode), a platinum electrode counter and $Ag/AgCl_2$ reference electrode. The protein was reduced by electrochemical potentials applied through EZStat Pro (Nuvant systems) potentiostat. The degree of FldA reduction was monitored spectrophotometrically with CARY WinUV-Vis spectrophotometer. In order to allow for the protein to stabilize, a total of 15 spectra were taken at one-minute interval each after every 30 mV decrease in the applied potential. The background absorbance due to the mediators was recorded by dissolving mediators to a final concentration of 10 μM in 50 mM MOPS buffer pH 7.0, in order to correct for baseline, before the spectra of the sample were recorded. Absorbance changes at 360 nm, 460 nm and 385 nm were followed relative to the reference wavelength at 700 nm. The potentials were corrected to those for standard hydrogen electrode (+186 mV) and plotted against the changes in absorbances at 385nm (sq/hq) and at 460 nm (ox/hq) by applying the Nernst equation incorporated in the Igor software.

Results and Discussion

$F_{420}H_2$-dependent electron bifurcation by $HdrA_2B_2C_2$ and electron transfer from $HdrA_2B_2C_2$ to the membrane-bound electron transport chain dependent on FldA or Fdx. Preparation of materials and assay protocols were as described previously (1). The initial rate of CoMS-SCoB reduction to the thiols HSCoM and HSCoB was nearly identical in reaction mixtures containing the heterodisulfide, $HdrA_2B_2C_2$, reduced coenzyme F_{420} ($F_{420}H_2$), and either FldA or Fdx (Fig. S6). Although at a reduced rate and final yield of thiols, the results establish that FldA is capable of replacing Fdx in the $F_{420}H_2$-dependent electron bifurcation by $HdrA_2B_2C_2$. Addition of everted membrane vesicles to the reaction mixtures enhanced the rate of heterodisulfide reduction and final yield of the corresponding thiols dependent on either FldA or Fdx. The results show that FldA is capable of mediating electron transfer from $HdrA_2B_2C_2$ to the membrane-bound electron transport chain culminating in reduction of CoMS-SCoB, although at a reduced rate and final yield of thiols compared to Fdx. The rate of CoMS-SCoB reduction and final yield of thiols was enhanced by the addition of NaCl to reactions containing either FldA or Fdx. This result is consistent with electron transport-coupled translocation of Na^+ from outside to inside vesicles supporting that FldA donates electrons to the Na^+-translocating Rnf complex. The rates shown in Figure 6 for FldA- and Fdx-dependent membrane-bound electron transport include minor contributions from $F_{420}H_2$ dehydrogenase-dependent membrane-bound electron transport to CoMS-SCoB, evidenced by results obtained with control reaction mixtures minus either $HdrA_2B_2C_2$ or FldA and Fdx. Nonetheless, the conclusions regarding the ability of FldA to replace Fdx are unaffected.

FIGURE S1. SDS-PAGE of purified recombinant FldA. Left lane, molecular mass markers. Right lane, loaded with 1µg of purified FldA. The gel was stained with Coomassie R-250.

FIGURE S2. Potentiometric titration of FldA. The changes in sq absorbance at 385 nm were plotted against the actual potentials experienced by the sample (mV). (A) The E_m for the ox/sq couple is -301 $\pm$ 5.06 mV. (B) The E_m for the sq/hq couple is -464 $\pm$ 2.61 mV. Conditions were pH 7.0 in 50 mM MOPS. The data in panels A and B were fitted separately using the modified Nernst equation (igor software) (2).

FIGURE S3. The three FldA protomers found in the asymmetric unit. The FldA proteins and FMN molecules are shown in ribbon and stick representations (cyan, protomer A; pink, protomer B; green, protomer C). Protomers A and B form a dimer and the promoter C also forms a dimer with a symmetry related protomer C shown as white ribbon and stick models.

FIGURE S4. Schematic of protein interactions with FMN of the FldA from *M. acetivorans*. Negative and positive charged atoms are shown in red and blue respectively. Hydrogen bonds are shown as purple lines with arrows. Lines in teal and lime green indicate polar and hydrophobic regions respectively. Green lines ending in dots indicate Pi-Pi stacking.

FIGURE S5. Pathway for conversion of acetate to methane in *M. acetivorans.* Ack, acetate kinase; Pta, phosphotransacetylase; CoA-SH, coenzyme A; H_4SPT, tetrahydrosarcinapterin; Fd_r, reduced ferredoxin; Fd_o, oxidized ferredoxin; Cdh, CO dehydrogenase/acetyl-CoA synthase; CoM-SH, coenzyme M; Mtr, methyl-H_4SPT:CoM-SH methyltransferase; CoB-SH, coenzyme B; MP, methanophenazine; Hdr-DE, heterodisulfide reductase; Rnf, Rnf complex; Mrp, Mrp complex; Atp, ATP synthase. Reproduced by permission (3).

FIGURE S6. $F_{420}H_2$-dependent electron bifurcation by $HdrA_2B_2C_2$ and electron transfer from $HdrA_2B_2C_2$ to the membrane-bound electron transport chain dependent on FldA or Fdx. The atmosphere was 100% N_2 and the temperature was 21°C for all reactions that were also initiated by addition of $F_{420}H_2$. The complete reaction mixture (300 µl) contained closed everted membrane vesicles (100 µg protein), 1.5 µM $HdrA_2$, 2 µM $HdrB_2C_2$, 200 µM CoMS-SCoB, 18 µM $F_{420}H_2$, 33 mM NaCl and either 5 µM Fdx or Fdx in 50 mM potassium phosphate buffer (pH 7.0). Complete: with Fdx (□); with FldA (■), with Fdx, minus NaCl (Δ); with FldA, minus NaCl (▲); with FldA, minus vesicles (▽); with Fdx, minus vesicles (▼); minus FldA or Fdx (◆); minus $HdrA_2B_2C_2$ (◇). There was no detectable increase in thiol content over the background level (1.2 µM) in the complete reaction mixture minus CoMS-SCoB or $F_{420}H_2$. Initial rates of thiol formation (µM/min) are indicated next to each reaction. Data points are the mean of three replicates for which the standard deviation is shown by error bars.

FIGURE S7. Distance tree of FldA and related proteins. The tree was constructed using the neighbor-joining method with significant alignments recovered from the NCBI database queried with FldA (MA1799) from *M. acetivorans*. The scale bar indicates the average number of amino acid substitutions per site. Flavodoxin sequences: WP_011021802.1, *Methanosarcina acetivorans*; WP_048183459.1, *Methanosarcina siciliae*; WP_048138299.1, *Methanosarcina horonobensis*; WP_048125136.1, *Methanosarcina lacustris*; WP_048118313.1, *Methanosarcina vacuolata*; WP_011307048.1, *Methanosarcina barkeri*; WP_048166050.1, *Methanosarcina thermophila*; WP_048088456.1 Candidatus *Methanoperedens nitroreducens*; WP_013194462.1, *Methanohalobium evestigatum*; WP_048198898.1, *Methanocella arvoryzae*; WP_013898822.1, *Methanosalsum zhilinae*; WP_013719833.1, *Methanosaeta concilii*; WP_015323860.1, *Methanomethylovorans hollandica*; WP_023845719.1, *Methanolobus tindarius*; WP_014406362.1, *Methanocella conradii*; WP_048146851.1, *Methanolobus psychrophilus*; WP_011022659.1, *Methanosarcina acetivorans*. WP_032279031.1, *Escherichia coli*; WP_027338967.1, *Halonatronium saccharophilum*; WP_011791702.1, *Desulfovibrio vulgaris*; WP_021760293.1, *Desulfovibrio gigas*; WP_015326202.1, *Halobacteroides halobius*; WP_002160966.1, *Bacillus cereus*;

WP_012058624.1, *Clostridium beijerinckii*. Lactamase sequences: WP_028323018.1, *Desulfatiglans anilini*; WP_0117
0051.1, *Syntrophobacter fumaroxidans*; WP_027177280.1, *Desulfovibrio hydrothermalis*.

FIGURE S8. Alignment of sequences from species in clades I and II, *Methanoperedens nitroreducens* and *Methanosaeta concilii.* Species correlating with the accession numbers are as shown in Fig. S7. Additional sequences are the generic flavodoxins from *M. acetivorans* (WP_011022659), *D. gigas* (WP_021760293) and *C. beijerinckii* (WP_012058624). The boxed sequences show sequence identity to the S_{56}TFYY$_{60}$ FMN binding motif of *M. acetivorans* FldA (WP_011021802).

Figure S1.

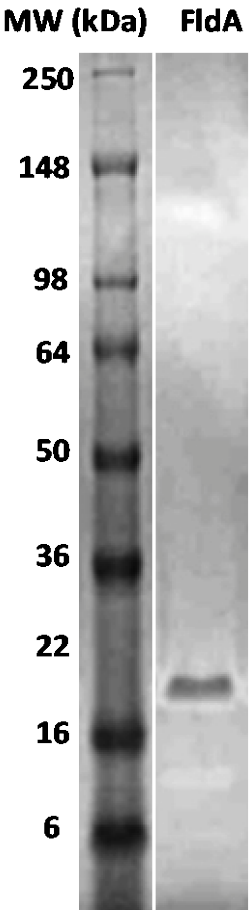

Figure S2.

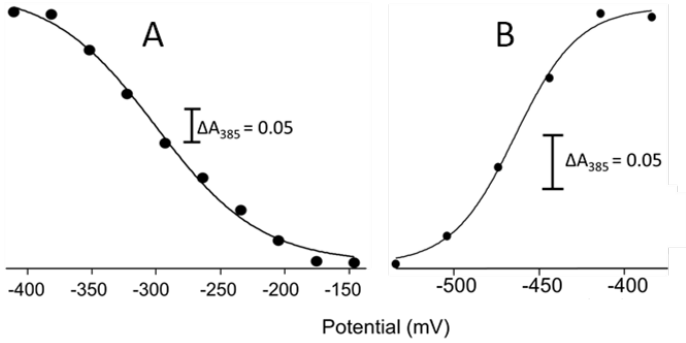

Figure S3.

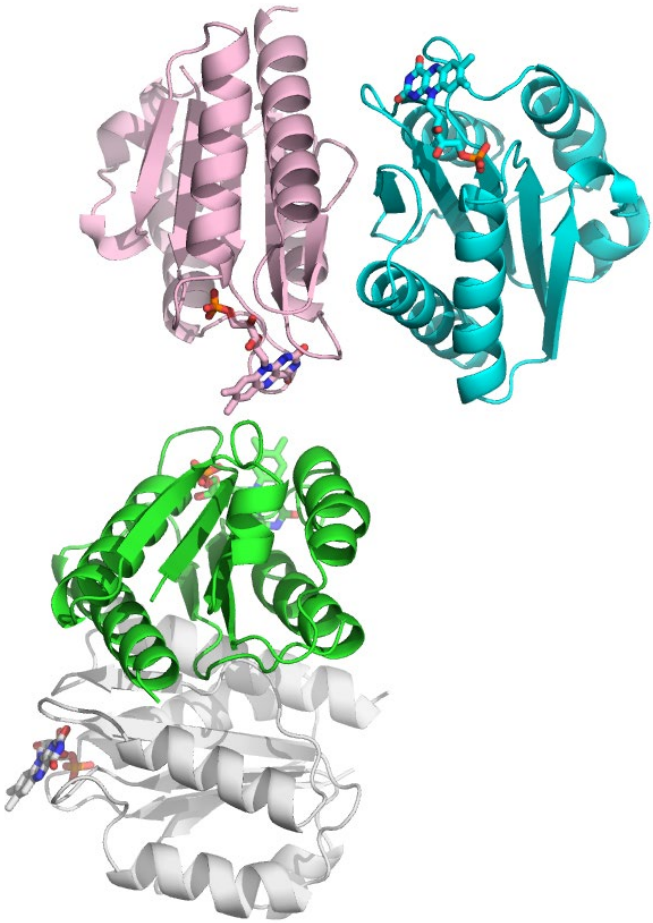

Figure S4

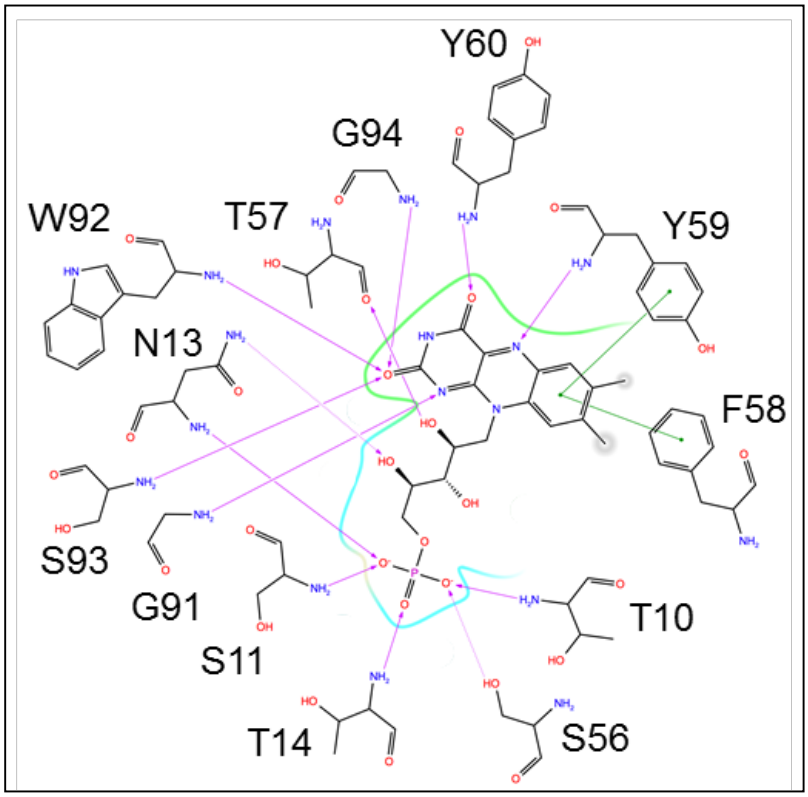

Figure S5

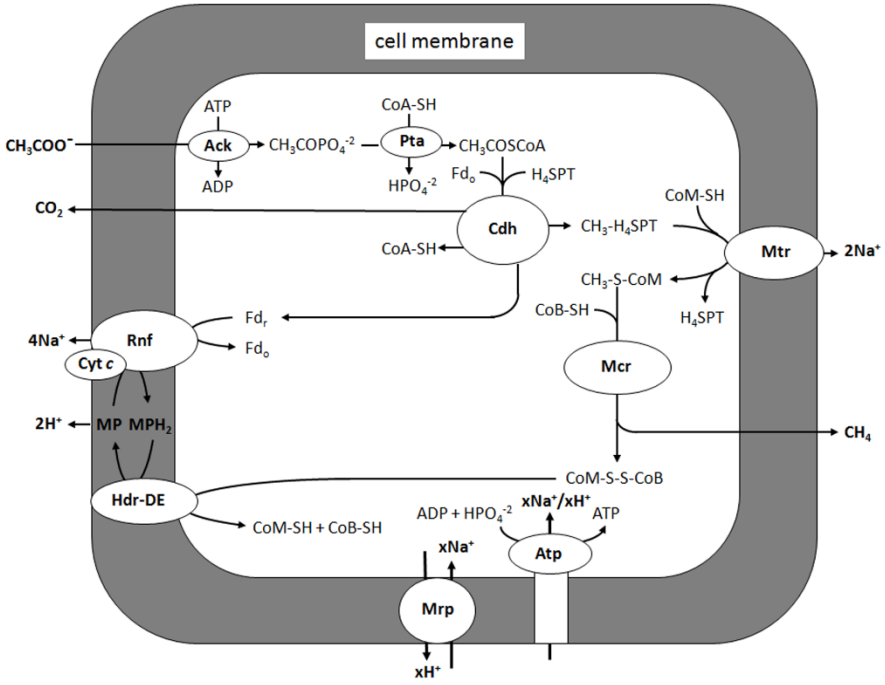
cell membrane
ATP
CoA-SH
CH_3COO^-
Ack
$CH_3COPO_4^{-2}$
Pta
$CH_3COSCoA$
ADP
HPO_4^{-2}
Fd_o
H_4SPT
CO_2
Cdh
CoM-SH
CH_3-H_4SPT
Mtr
$2Na^+$
CoA-SH
CH_3-S-CoM
CoB-SH
H_4SPT
Fd_r
$4Na^+$
Rnf
Fd_o
Cyt *c*
Mcr
$2H^+$
MP MPH_2
CH_4
CoM-S-S-CoB
Hdr-DE
$ADP + HPO_4^{-2}$
xNa^+/xH^+
ATP
CoM-SH + CoB-SH
xNa^+
Atp
Mrp
xH^+

Figure S6

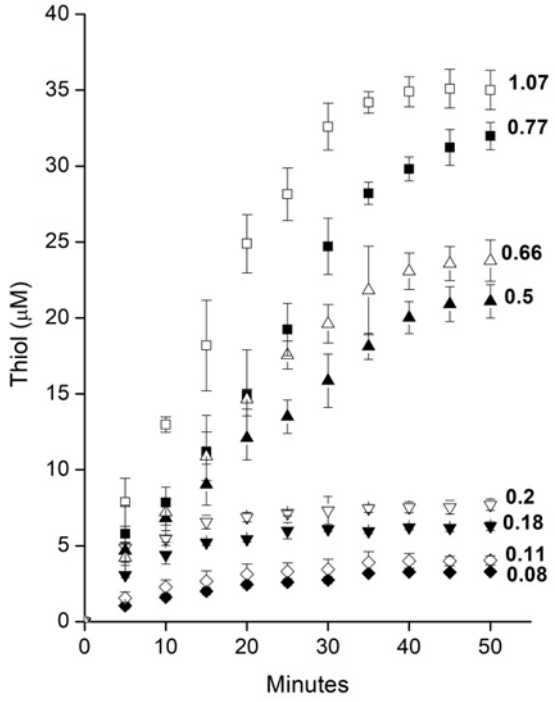
Thiol (μM)
Minutes
0
5
10
15
20
25
30
35
40
0
10
20
30
40
50
1.07
0.77
0.66
0.5
0.2
0.18
0.11
0.08

Figure S7

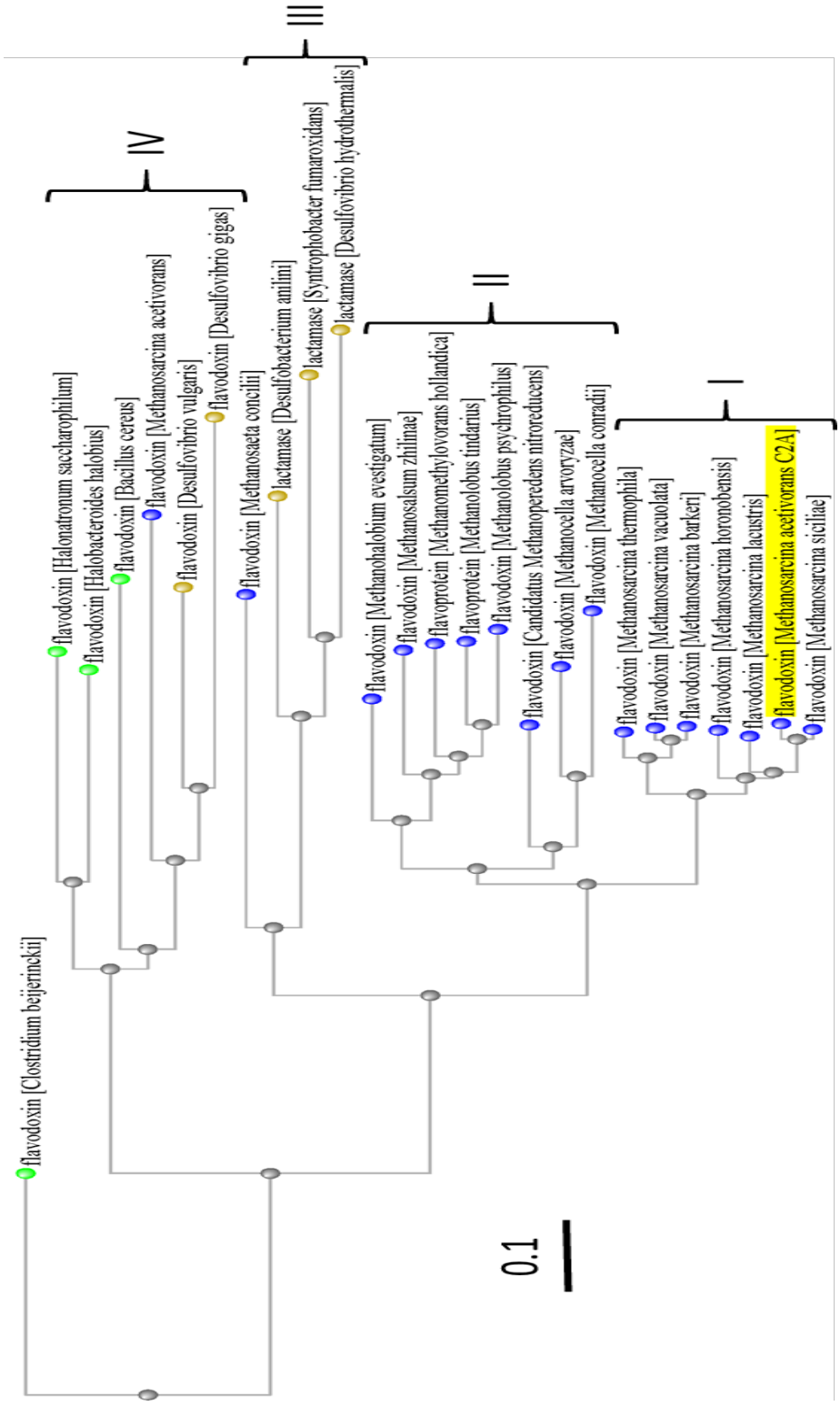
flavodoxin [Clostridium beijerinckii]
flavodoxin [Halonatronum saccharophilum]
flavodoxin [Halobacteroides halobius]
flavodoxin [Bacillus cereus]
flavodoxin [Methanosarcina acetivorans]
flavodoxin [Desulfovibrio vulgaris]
flavodoxin [Desulfovibrio gigas]
flavodoxin [Methanosaeta concilii]
lactamase [Desulfobacterium anilini]
lactamase [Syntrophobacter fumaroxidans]
lactamase [Desulfovibrio hydrothermalis]
flavodoxin [Methanohalobium evestigatum]
flavodoxin [Methanosalsum zhilinae]
flavoprotein [Methanomethylovorans hollandica]
flavoprotein [Methanolobus tindarius]
flavodoxin [Methanolobus psychrophilus]
flavodoxin [Candidatus Methanoperedens nitroreducens]
flavodoxin [Methanocella arvoryzae]
flavodoxin [Methanocella conradii]
flavodoxin [Methanosarcina thermophila]
flavodoxin [Methanosarcina vacuolata]
flavodoxin [Methanosarcina barkeri]
flavodoxin [Methanosarcina horonobensis]
flavodoxin [Methanosarcina lacustris]
flavodoxin [Methanosarcina acetivorans C2A]
flavodoxin [Methanosarcina siciliae]
IV
III
II
I
0.1

Figure S8.


WP_011021802 1 M---KAIVVYLSTSGNTKAMAEAIGNGIES-KNVDVQVISFYDVKLD-ELKEAEAIAVGSSTFYYKMLLPM--EKFMD-- 71
WP_048183459 1 M---KAIVVYLSTSGNTKAMAEAIGNGIES-KNVDTKVVSFYDVKLE-ELKEAEAIAVGSSTFYYKMLLPM--EKFMD-- 71
WP_048138299 1 M---KAIVVYLSTSGNTKVMAEAIGNGIES-KNVDVKVVSFYDVKPE-ELNEAEAIAIGSSTFYYKMLLPM--EKFMN-- 71
WP_048125136 1 M---KAIVVYLSTSGNTKDMAEAIGKGIES-KNVDVKVISFYDVKPE-ELNEAEAIAVGSSTFYYKMLLPM--EKFMN-- 71
WP_048118313 1 M---KAIVVYLSTSGNTKAMAEAIASGIES-KHVDAKAISFYDVKLE-DLYEADAIAVGSSTFYYRMLQPM--EKFMD-- 71
WP_011307048 1 M---KAIVVYLSTSGNTKAMAEAIASGIES-KHVDAKAISFYDVKLE-DLNEADAIAVGSSTFYYRMLQPM--EKFMD-- 71
WP_048166050 1 M---KAIVVYLSTSGNTKIMAEAIASGIES-KHVDAKAVSFYDVKVE-DLNEADAIAVGSSTFYYKMLQPM--EKFMD-- 71
WP_048088456 1 M--pKVVIVYLSTSGNTKAMADAIAEGVRS-RNVEALAVNFHEADIE-DLRSADAIAIGSSTFYYKMLPPM--EKFI--- 71
WP_013194462 1 M--aKLAVVYLSTQGNTKTMAESIANGAKS-RHVDVDVSSFYDTTVD-EVAAADAIAIGSSTFYYGMLAPI--EKFVD-- 72
WP_048198898 1 ------MVVYLSTSGNTKRMADAIAAGADS-RGINSEVVSFYDVDLD-KLRSADAIAIGSSTFWYKMHDAM--EKFLDr- 69
WP_013898822 1 M--pKLAIVYLSTQGNTMLMAEGIAEGAIS-RNIDVEVRSFYEWNPM-DAASADGIAVGSSTFNYAMHPPI--QKFL--- 71
WP_013719833 1 M--pKIAIIYASQSGKTKRMAEAIANGAKSvEGVDVLLKNVFQAKPD-DVLDADAVVLGGSTYNSKLIKTM--DPFLA-- 73
WP_015323860 1 M--vKLAIVYLSTQGSTRMMAEAIAEGARQ-KHIEVRVDSFYEWEPK-DAASYDGIAVGSSTFYYKMLEPI--SKFL--- 71
WP_023845719 1 M--pKLAIVYLSTQGSTKMMAEAIAEGARE-KHVDVDIDNFYEWDPA-EVAKYDAICIGSSTFYYTMLEPI--AKFL--- 71
WP_014406362 1 MvkpKLVVVYLSTQGNTKKMADAIAHGAED-RGMEARSVSFYEADMN-EIRDADAIALGSSTFWYKMHDAM--ERFIErm 76
WP_048146851 1 M--pKLAIVYLSTQGNTQMMAEAIAEGARE-RHVEVKVNNFHEWNPA-EIADYDAIAVGSSTFYYTMLDPI--AKFI--- 71
WP_011022659 1 Me--KTIIVYGSSTGNTEILAEEIKGTLEK-YDGKVKLMEVTDLHPT-DLANYDTILLGCSTWGDGELQDD--FIPFE-- 72
WP_021760293 1 M--pKALIVYGSTTGNTEGVAEAIAKTLNS-EGMETTVVNVADVTAPgLAEGYDVVLLGCSTWGDDEIELQ--EDFVPl- 74
WP_012058624 1 -----MKIVYWSGTGNTEKMAELIAKGIIE-SGKDVNTINVSDVNID-ELLNEDILILGCSAMGDEVLEESefEPFIE-- 71
WP_011021802 72 -ETLVASNPQGKIGAAFGSYGWSGEA PILIAEKMREMGMTVMDPVLRILHKPTDKDLQECKRLGIDIAEKVKHKGTK 147
WP_048183459 72 -ETLVASNPQGKIGAAFGSYGWSGEA PILIAEKMREMGMTVMDPVLRILHKPTDKDLQECKRLGIDIAEKVKHKSTK 147
WP_048138299 72 -ETLVSTNPQGKLGAAFGSYGWSGEA PIMIAEKMRELGMTVMDPVLRILHRPTDKDLQECKRLGVDIAEKMKQRSKK 147
WP_048125136 72 -ETLISANPQGKIGAAFGSYGWSGEA PILIAEKMREMGMSVVDPVLRILHKPTDKDLQECKRLGIDIAEKLKHKSKK 147
WP_048118313 72 -ETLVSTNPKGKLGAAFGSYGWSGEA PILIAEKMRDMGMTVIDPVLRILHKPTDKDIQECKRLGVDIAEKLKHKSSK 147
WP_011307048 72 -EILASTNPKGKLGAAFGSYGWSGEA PILIAEKMRDMGMTVIDPVLRILHKPTDKDLQECKRLGVDIAEKLKHRSSK 147
WP_048166050 72 -ETLASTNPKGKLGAAFGSYGWSGEA PILIAEKMREMGMIVIDPVLRILHKPTDKDVQECKRLGVDIAEKMKQ-ISK 146
WP_048088456 72 -ENLAREDVKEKIGAAFGSYGWSGEA PVMIAEKMREIGMKVIDPVLRIQYTPTDKDLEECKRLGKDIAIRLKAK--- 144
WP_013194462 73 --ELVQKDVDGKIGAAFGSYGWSGEA PHMIADKMRKAGMNVVDPVLRIQHIPNDKDISECERLGKDLAENIKKR--- 144
WP_048198898 70 ---LKPLKLEGKVGAAFGSYGWSGEA PVQIAQKMRELGLDVIDPVLRVQWDPEEKDLKECERLGKDIAKALKKEPVP 143
WP_013898822 72 -DQMLETEVKGKIGAAFGSYGWSGEA PVMIADKMRKAGMNVIDPVLRIQYRPTEKDIAECVRLGKDLAEKIKHNK-- 145
WP_013719833 74 --QLEKLDLKGKVGVAFGSYGWSGEG VPILIDRMKSFGMSVIEPGTTAVQLPTKEDLERCTDLGKAVANGLLN---- 144
WP_015323860 72 -DALIAEGVEGKVGSAFGSYGWSGEA PVIIAEKMREAGMKVIDPVLRIQYIPEEKDIKECQRLGKDIAIKLKKLVTE 147
WP_023845719 72 -DKLIEIGIEGKLGAAFGSYGWSGEA PVLIAEKLRKAGVEVIDPVLRIQYVPNEKDLAECIRLGKDMAKKMKKKE-- 145
WP_014406362 77 gKELGQTAIEGKVGAAFGSYGWSGEA PVDIARMMRSLGIKVIDPVLRVQYEPNERDLEECKRLGKDIANAVKKTVRP 153
WP_048146851 72 -DRIVEVGVDGKIGAAFGSYGWSGEA PVKIAEKLRNAGVEVIDPVLRIQYTPTEKDLFECNRLGKDLAERMKNR--- 144
WP_011022659 73 -EEMEGVDLKGKKAACFGPGDSTFPL[4]VDLLEEKLKSCGAQIIVEGLKIDGD-VDYQLDKAEEWANEVAQAVSV---- 147
WP_021760293 75 yEDLDRAGLKDKKVGVFGCGDSSYTY[4]VDVIEKKAEELGATLVASSLKIDGEPDSAEV-------LDWAREVLARV-- 146
WP_012058624 72 --EIST-KVSGKKVALFGSYGWGDGK[1]MRDFEERMNAYGCVVVETPLIVQNEPDEAE-QDCIDFGKKIANI------- 138

TABLE S1: Data collection and refinement statistics of the *M. acetivorans* FldA.

[a]Data collection		Refinement	
Wavelength (Å)	0.9181	Resolution (Å)	27.09-1.68
Resolution (Å)	50-1.68	R_{work}/R_{free} (%)	18.0/ 20.7
No. of Reflections	1,514,263/73,408	B-factors	
(tot./uni.)		Protein	23.110
Completeness (%)	98.1 (88.7)[c]	Ligand	16.968
$I/\sigma(I)$	30.3 (2.6)[c]	Water	30.716
[b]R_{sym} (%)	6.9 (57.4)[c]	R.m.s deviations	
		Bond lengths (Å)	0.035
		Bond angles (°)	2.612

[a]Data set was collected by synchrotron radiation (F1 line) at the MacCHESS (Cornell University, Ithaca, NY).

[b]$R_{sym} = \sigma|I - \langle I \rangle|/\sigma I$, where I is observed intensity and $\langle I \rangle$ is average intensity obtained from multiple observations of symmetry related reflections.

[c]Highest resolution shell (1.71-1.68 Å) is shown in parenthesis.

Bibliography

1. Yan Z, Wang M, & Ferry JG (2017) A Ferredoxin- and $F_{420}H_2$-dependent, electron-bifurcating, heterodisulfide reductase with homologs in the domains *Bacteria* and *Archaea*. *mBio* 8:e02285-02216. doi: 02210.01128/mBio.02285-02216.
2. Ferlez B*, et al.* (2016) Thermodynamics of the electron acceptors in *Heliobacterium modesticaldum*: an exemplar of an early homodimeric type I photosynthetic reaction center. *Biochemistry* 55(16):2358-2570.
3. Suharti S, Wang M, de Vries S, & Ferry JG (2014) Characterization of the RnfB and RnfG subunits of the Rnf complex from the archaeon *Methanosarcina acetivorans*. *PLoS One* 9:e97966.